Journal of Applied Polymer Science

Interfacial Polymerization of Poly(2,5-dimethoxyaniline) and Its Enhanced Capacitive Performances

Shanxin Xiong,[1,2] Yujing Shi,[1] Shi Chen,[1] Jie Li,[1] Xiaoqin Wang,[1] Jia Chu,[1] Ming Gong,[1] Bohua Wu[1]

[1]College of Chemistry and Chemical Engineering, Xi'an University of Science and Technology, Xi'an 710054, People's Republic of China

[2]State Key Laboratory of Polymer Materials Engineering, Sichuan University, Chengdu, 610065, People's Republic of China

Correspondence to: S. Xiong (E-mail: xiongsx689@sohu.com)

ABSTRACT: The poly(2,5-dimethoxyaniline) (PDMA) were synthesized through interfacial polymerization method using three various organic solvent/water reaction systems. As comparison with conventional chemical polymerized PDMA, the interfacial polymerization can produce uniform nanoparticular PDMA, especially for using high density (higher than water) solvent as organic phase. The capacitive performances of interfacial polymerized PDMA can be benefited from its uniform morphologies and loose packing structure. The specific capacitance of interfacial polymerized PDMA using carbon tetrachloride is 194 Fg^{-1} at current density of 50 mA cm^{-2}, which has 59% enhancement over 122 Fg^{-1} of conventional PDMA at the same current density. The energy density of interfacial polymerized PDMA is 39 Wh kg^{-1} at current density of 5 mA cm^{-2} and the power density is 28,421 W kg^{-1} at current density of 50 mA cm^{-2}. The energy density has improvement in different extent as comparison with that of conventional PDMA. The enhanced capacitive performances can be attributed to the increased ionic conductivity induced by the loose molecular packing structure and uniform morphology produced by the interfacial polymerization process. © 2014 Wiley Periodicals, Inc. J. Appl. Polym. Sci. **2014**, *131*, 40666.

KEYWORDS: conducting polymers; electrochemistry; surfaces and interfaces

Received 1 November 2013; accepted 2 March 2014

DOI: 10.1002/app.40666

INTRODUCTION

Attributing to the high specific capacitance of conducting polymer resulting from the high exchangeable charge during their reversible redox reactions, the conducting polymer-based supercapacitor electrode materials have attracted wide interest of researchers in the energy storage fields. Among of the conducting polymers, polyaniline (PANI) has been intensively studied because of its high specific capacitance, ease in preparation and low cost.[1,2] Although the capacitance of PANI is mainly contributed by its redox reaction, the morphology and microstructure of PANI also play the important role in determination of its capacitive performances. The nanostructural PANI normally produces high capacitive properties. It may attribute to the fast redox reactions brought by large interfacial area with electrolytes, short diffusion length of ions and more accessible redox sites during the charge–discharge process.[3] Recently, a series of conducting polymer nanostructures including nanotubes, nanowires, and nanoparticles have been prepared and used in various fields including supercapacitor electrodes. Raghu[4] synthesized the MWCNTs-core/thiophene polymer-sheath composite nanocables by a cationic surfactant-assisted chemical oxidative polymerization for varied applications. Wang[5] synthesized successfully the PANI nanofiber by electrochemical method with very high specific capacitance of 1.21×10^3 Fg^{-1}. The pulsed sonoelectrochemical method was used in Gedanken's work[6] to prepare PANI nanoparticle with size of 20–40 nm. The specific capacitance is 166 Fg^{-1}. Li[7] also synthesized PANI nanowires with diameter of 30 nm through membrane template route. The capacitance of PANI nanowires arrayed electrode is 1142 Fg^{-1} at current density of 5 Ag^{-1}. The electrospun PANI nanofiber with specific capacitance of 267 Fg^{-1} is reported in Srinivasan's work.[8] Though the specific capacitances of PANI are varied in a large range according to the different preparation methods, a general feature is that the nanostructural PANI with high aspect ratio give high specific capacitance.

Interfacial polymerization is one of effective routes for preparation of conducting polymer nanostructrues, which has easy control, large-scale production, and low cost features. Huang[9–11] has prepared successfully the PANI nanowires using interfacial polymerization process. The resultant materials possess even structures and uniform morphologies. Prakash[12–14] also utilizes the interfacial polymerization technique for preparation of various

structures (hollow microspheres and nanotubes) of polycarbazole, polyindole, and polyanthranilic acid. The interfacial polymerization method supplies a highly effective approach for preparation of nanoelectrode materials in large scale. It can also be utilized for preparation of PANI nanofiber supercapacity electrode.[15] Although PANI is widely utilized as supercapacitor electrode materials, the capacitive properties of its derivatives are studied seldom.[16] As one of the PANI derivatives, the poly(2,5-dimethoxylaniline) (PDMA) possesses better processability and high activity as comparison with PANI owing to the stereo-specific blocking effect and electron-donor function of its two methoxyl groups. It will be interested to study the capacitive performance of PDMA. Furthermore, PDMA can be synthesized by the interfacial polymerization method to produce novel nanostructures. With consideration of the unique molecular growth process in the interfacial polymerization and the contribution of large specific surface area and high electrochemical activity of conducting polymer nanostructure, it is reasonable to believe that the interfacial polymerization will bring novel structure and high capacitive performance to PDMA. Herein, we synthesize two kinds of PDMA using conventional chemical polymerization and interfacial polymerization methods, respectively. The comparison study of structure, morphologies and capacitive properties were carried out between these two kinds of PDMA.

EXPERIMENTAL

Chemical Polymerization of PDMA

All chemicals are analytical reagent and used as received unless otherwise specified. In a typical experimental, the monomer 2,5-dimethoxylaniline (DMA) and the oxidant agent ammonium peroxydisulfate (APS) with molar ratio of 1/2 were dissolved in 25 mL and 5 mL 1*M* HCl solution, respectively. The APS/HCl solution was dropped into DMA/HCl solution with stir in three separate doses in 30 min. The reaction was carried out for 24 h at room temperature. The resultant product was washed with acetone and deionized water for three times to remove the unpolymerized monomer and sulfate salts and dried at 40°C in vacuum oven overnight. The final product was denoted as PDMA-n.

Interfacial Polymerization of PDMA

In a typical experimental, 1.6 mmol DMA was dissolved in 10 mL of xylene, chloroform, and carbon tetrachloride, respectively as organic phase. Various amounts (0.4 mmol, 0.6 mmol, and 0.8 mmol) of APS were dissolved in 10 mL 1*M* HCl solution as water phase. The addition sequences of reagents are determined by the density difference of organic solvent and water, which obey the principle of high density materials first. For xylene/water system, the water phase was added into the vial first, and then the organic phase was added carefully on the top of water phase to avoid breaking the steady state of interface. For chloroform/water and carbon tetrachloride/water systems, the organic phases were added into the vial first, and then the water phase was added carefully on the top of organic phase. The vial was standed vertically for 24 h for the proceeding of reaction. After the organic phase was removed, water phase was filtered and washed with acetone and deionized water for three times to remove the unpolymerizaed monomer and sulfate salts. The final products were dried at 40°C in vacuum oven overnight. The final products were denoted as PDMA-x, PDMA-c, and PDMA-t for materials using xylene, chloroform, and carbon tetrachloride as organic phases, respectively.

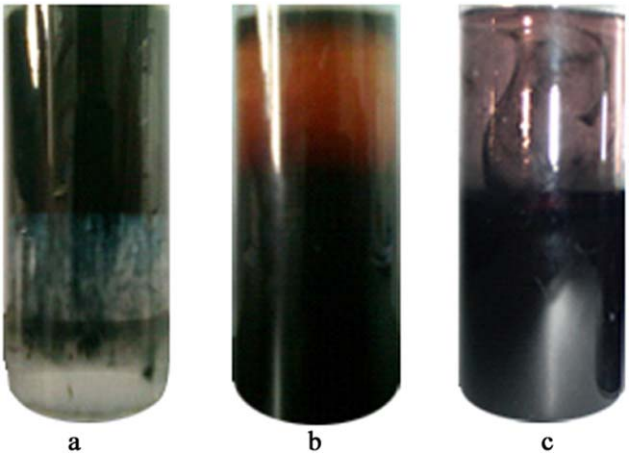

Figure 1. Experimental phenomena of interfacial polymerization of PDMA using xylene (a), chloroform (b), and carbon tetrachloride (c) as organic phases, respectively. Photograph is recorded in 10 s after adding the second phase. [Color figure can be viewed in the online issue, which is available at wileyonlinelibrary.com.]

Fabrication of Supercapacitor Electrode

The mixture of PDMA, conducting carbon black and PTFE aqueous suspension with weight ratio of 75 : 20 : 5 were dispersed in ethanol with assistance of grind and ultrasonic treatment. The mixture was casted even on a graphite paper electrode to form a thin film with area of 1 cm^2 and weight of ~0.5 mg. The electrode was dried at 50°C overnight.

Characterization

Fourier transform infrared (FTIR) spectra of the materials were obtained on a PerkinElemer GX Spectrometer using KBr pellet method. The morphologies of PDMA were observed on a JSM-6460LV scanning electron microscope. The pore size distribution was obtained on a Micromeritics ASAP 2020 Physisorption Analyzer. All of the electrochemical tests were carried out using AUTOLAB PGSTAT302N potentiostat. The cyclic voltammetry (CV) and charge–discharge experiments were performed using Pt plate (99.99%) and Ag/AgCl (3M KCl) as counter and reference electrodes, respectively, in a 1*M* H_2SO_4 solution.

RESULTS AND DISCUSSION

Interfacial Polymerization of PDMA

The interfacial polymerization of PDMA is occurred at the interface of organic phase and water phase. The monomer in the organic phase was oxidized by the APS from the water phase at their interface, and then diffused into the water phase. Because of lack of monomer in the water phase, once the PDMA is entered into water phase, the growth process of PDMA will stop. So the size and the morphology of interfacial polymerized PDMA is different from those synthesized by the conventional chemical polymerization, in which the growth will not stop until all of the monomer are run out. According to the different growth processes, the morphologies of resultant products may be variable,

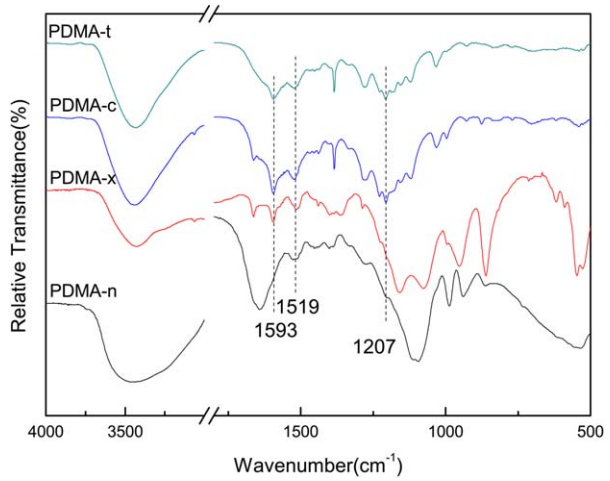

Figure 2. FTIR spectra of PDMA synthesized by conventional chemical polymerization (PDMA-n) and interfacial polymerization with various organic/water systems (PDMA-x, PDMA-c, and PDMA-t). [Color figure can be viewed in the online issue, which is available at wileyonlinelibrary.com.]

e.g., nanotubular structure of PANI. To investigate the interfacial polymerization process of PDMA, we chose three kinds of organic solvents with different densities as organic phases. Figure 1 shows the experimental phenomena of PDMA diffusing from organic phase into water phase during the initial period of interfacial polymerization. In xylene/water system [Figure 1(a)], due to its low density of xylene, the organic phase is on the top of the water phase. Just after the organic phase was added, some blue materials diffused into the water phase, indicating the formation of PDMA. The experimental phenomena of chloroform/water and carbon tetrachloride/water systems [Figure 1(b,c)] are similar. The produced PDMA was diffused from organic phase into above water phase. At the same time, the water solution became brown color. With on-going of polymerization, the whole reaction system was converted to dark brown color, which verifies that the PDMA can be synthesized successfully with these three organic solvent/water systems. With adding various amount of APS, the experimental phenomena does not show any difference.

Structures and Morphologies of PDMA

FTIR spectra of conventional PDMA synthesized by chemical polymerization and interfacial polymerized PDMA were used to study the structure difference of PDMA as shown in Figure 2. It can be seen that though the peak intensities of four FTIR spectra are different, the main characteristic peaks of PDMA are appeared in all four spectra. The broad band at 3441 cm^{-1} is assigned to the N—H stretching vibration. The C═N and C═C stretching modes for the quinoid (Q) and benzoid (B) rings of PDMA occur at 1593 cm^{-1} and 1519 cm^{-1}, respectively. The band at 1207 cm^{-1} is assigned to the presence of *o*-methoxy groups of PDMA,[17] which confirm the successful polymerization of PDMA. In the FTIR spectrum of PDMA-n, due to the neighbouning strong absorption of 1639 cm^{-1}, the C═N peak (Q) is exhibited as a shoulder peak. Furthermore, the PDMA-c and PDMA-t exhibit almost same FTIR spectra, which should relate to that the similar organic solvent of chloroform and carbon tetrachloride are used for their synthesis.

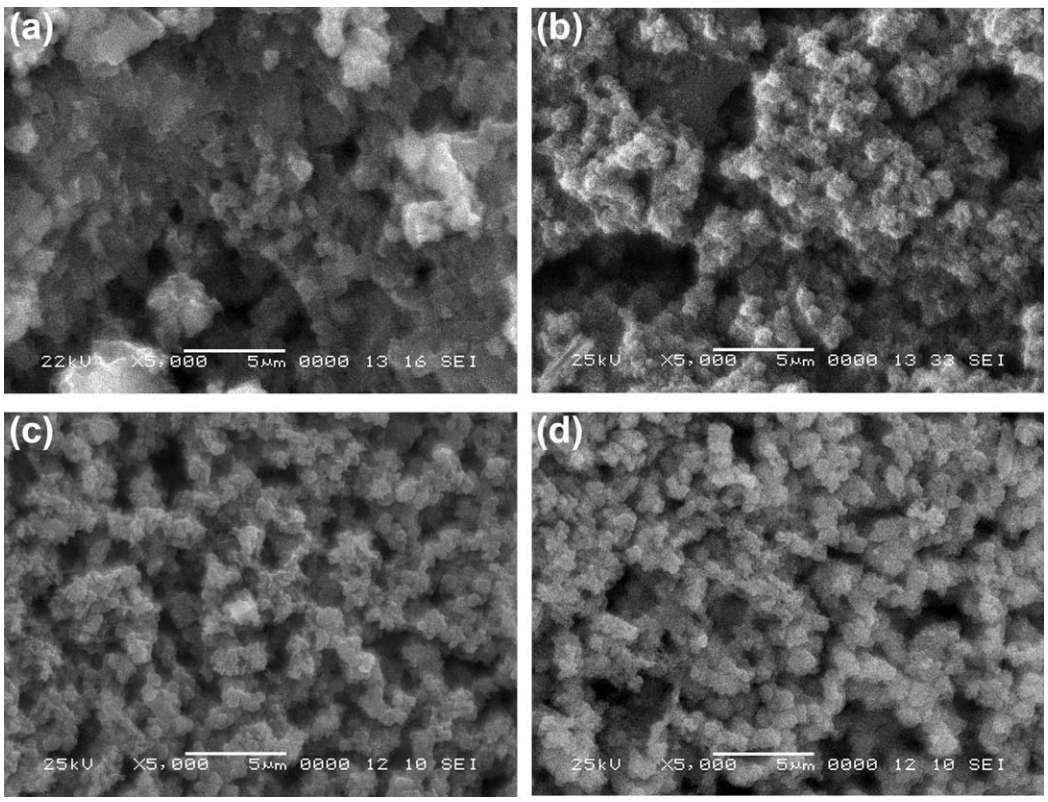

Figure 3. Morphologies of PDMA synthesized by conventional chemical polymerization (a), and interfacial polymerization using xylene (b), chloroform (c), and carbon tetrachloride (d) as organic solvents, respectively.

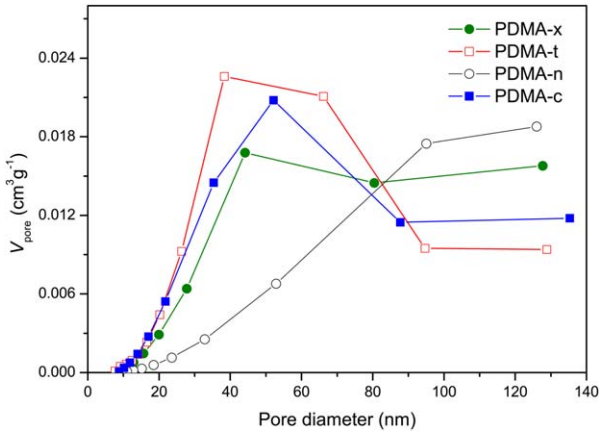

Figure 4. Pore size distribution of PDMA-n, PDMA-x, PDMA-c, and PDMA-t. [Color figure can be viewed in the online issue, which is available at wileyonlinelibrary.com.]

The morphologies of four kinds of PDMA are shown in Figure 3. It can be seen that the PDMA-n is consisted of particle with various size from several hundred nanometers to several micrometers and the aggregation of the particle is serious, while the interfacial polymerized PDMA exhibits a relatively uniform morphology. However, the interfacial polymerized PDMA shows a particle shape, which is totally different from the nanofiber morphologies of interfacial polymerized PANI. Reference to Huang's mechanism,[9–11] the difference between interfacial polymerization and conventional chemical polymerization is that the PANI nanofiber formed by rapid oxidative reaction of monomer in the initial stage of polymerization cannot act as the nucleation centre for further growth of molecule in two separated phases of interfacial polymerization system due to lack of continuous supply of monomer. In one word, the subsequent secondary growth of molecular chain is forbidden in the interfacial polymerization by the two separated phases. In our case, the easy oxidation feature of DMA caused from the electron-donor function of its two methoxy groups results in very fast growth of PDMA. So even in the short contact time of monomer and oxidant agent at the interface, the secondary growth of PDMA on its initial nanostructure is occurred. But with employing different organic solvents, the morphologies of PDMA are various. Among of three organic solvent/water systems, the PDMA synthesized using xylene/water system shows severe aggregation and its particle size is not even. Owing to similar solvent properties of chloroform and carbon tetrachloride, the PDMA-c and PDMA-t exhibit alike morphologies except that the particle size distribution of PDMA-t is uniform than that of PDMA-c. The similar structure was also confirmed by their alike FTIR spectra. The morphology difference of three systems may relate to the density difference of organic solvents

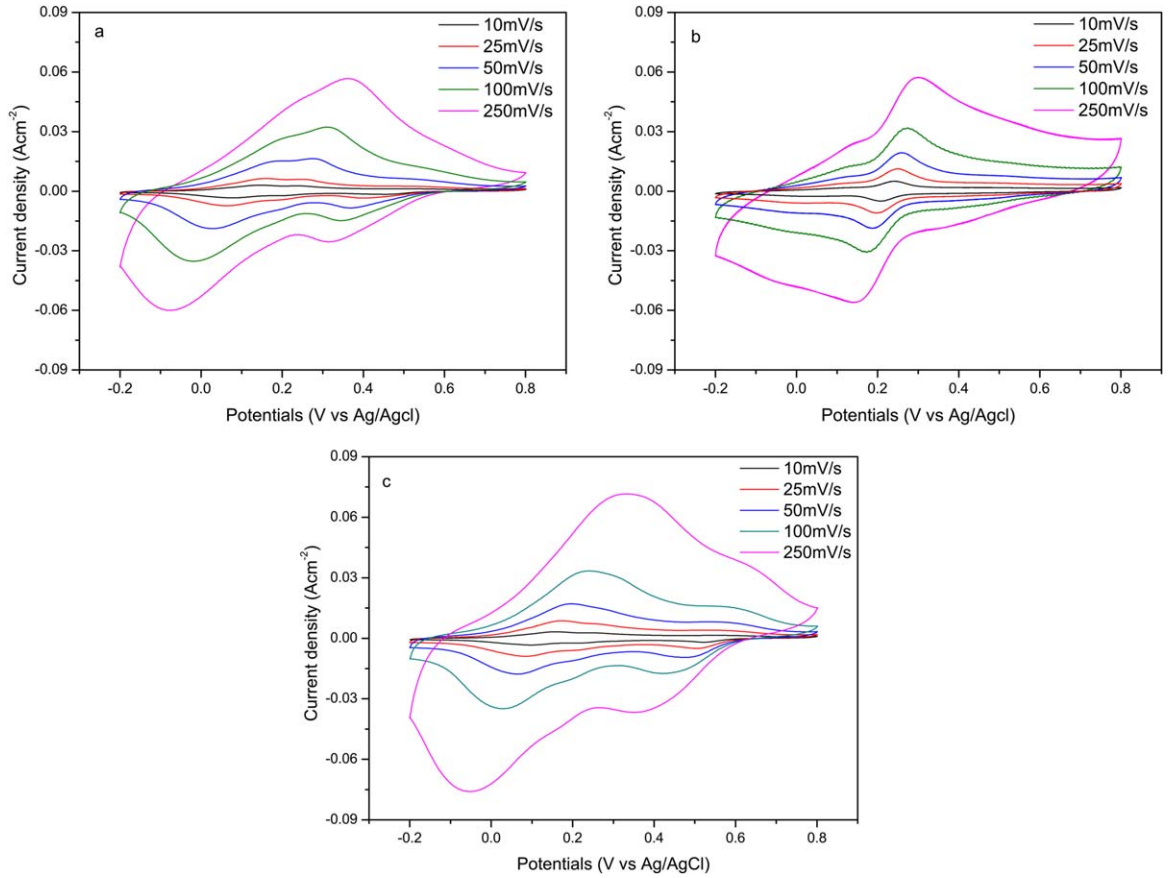

Figure 5. CV curves of PDMA-n (a), PDMA-x (b), and PDMA-t (c) measured in 1*M* H_2SO_4 solution with scan rate of 10, 25, 50, 100, and 250 mV s^{-1}, respectively using Ag/AgCl (3*M* KCl) reference electrode and Pt counter electrode. [Color figure can be viewed in the online issue, which is available at wileyonlinelibrary.com.]

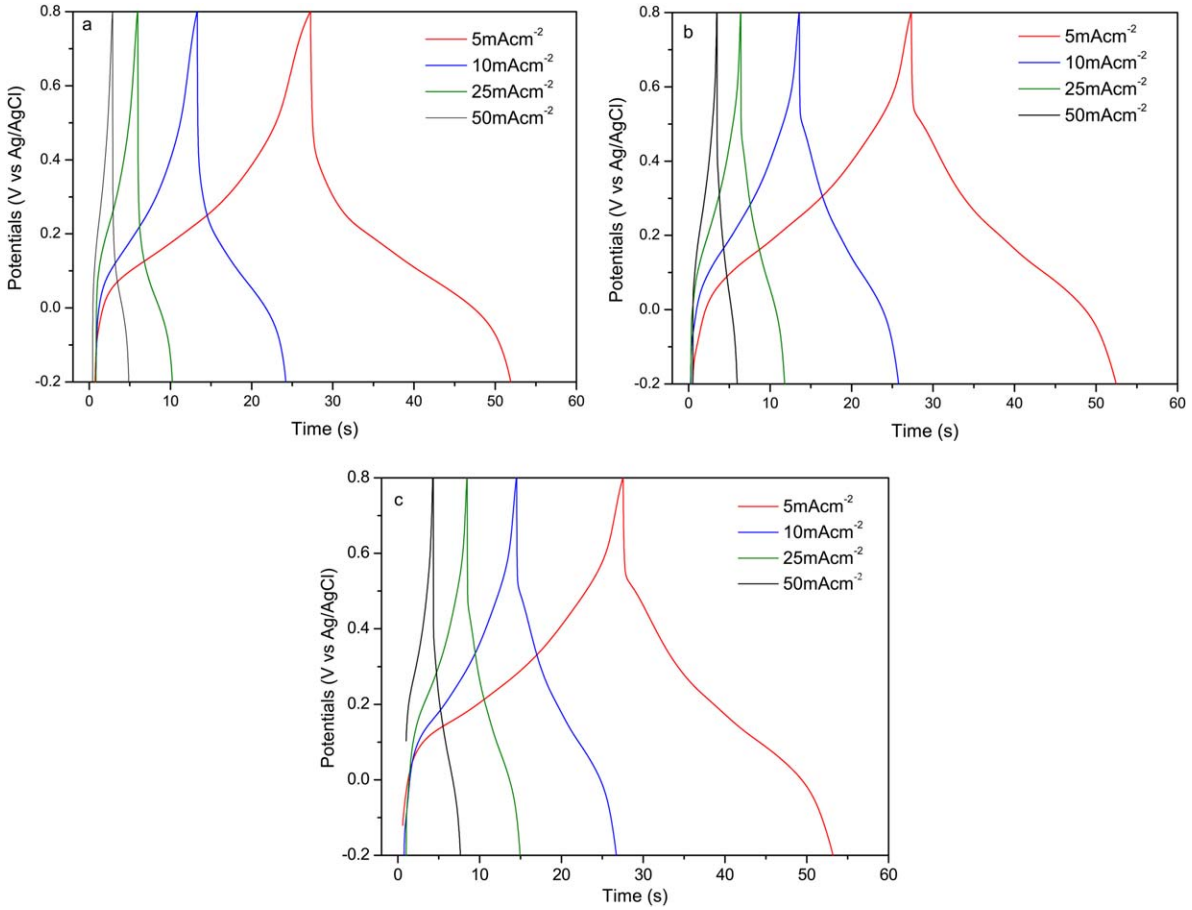

Figure 6. Charge–discharge curves of PDMA-n (a), PDMA-x (b), and PDMA-t (c) at different current densities of 5, 10, 25, and 50 mA cm^{-2}, respectively in 1*M* H_2SO_4 solution. [Color figure can be viewed in the online issue, which is available at wileyonlinelibrary.com.]

used. In xylene/water system, the organic phase is on the top of water phase, all of synthesized PDMA with different size are deposited in the water phase, resulting in complex morphologies. In another two systems, the organic phase are at the bottom of water phase, only light PDMA particle with suitable size range are floated in water phase. Also, the pore size test shows that these four PDMA possess various pore sizes and distribution. As shown in Figure 4, the PDMA-n is mainly consisted of meso- and macropores and the macropores domain the pore volume, while the PDMA-x, PDMA-c, and PDMA-t are consisted of micro-, meso-, and macropores and the mesopores domain the pore volume. The mesopores pore volume can follow a sequence of PDMA-t > PDMA-c > PDMA-x. The relatively higher mesopores pore volume can supply large specific surface area and more ion pathway, which may favor the charge–discharge process. With consideration of similar size, morphology, and structure of PDMA-c and PDMA-t, only PDMA-n, PDMA-x and PDMA-t are employed for the comparison study of the capacitive performances in this article.

Table I. Capacitive Performance of PDMA-n, PDMA-x, and PDMA-t at Different Current Densities

	Current density (mA cm^{-2})	Specific capacitance (Fg^{-1})	Specific energy density (Wh kg^{-1})	Specific power density (W kg^{-1})
PDMA-n	5	275	38	5338
	10	227	31	10,182
	25	139	20	17,142
	50	122	17	30,600
PDMA-x	5	277	38	5,472
	10	239	33	9,810
	25	153	22	14,776
	50	152	22	30,817
PDMA-t	5	281	39	5,484
	10	246	34	10,200
	25	199	28	15,508
	50	194	27	28,421

Capacitive Performances of PDMA

The electrochemical redox behaviors of two types of PDMA were studied by CV analysis. Figure 5 shows the CV curves of PDMA-n, PDMA-x, and PDMA-t with different scan rate from 10 mV s^{-1} to 250 mV s^{-1}. It can be seen that PDMA-n, PDMA-x, and PDMA-t exhibit reversible switching even at the high scan rate of 250 mV s^{-1}. Two pairs of redox peaks appear in two samples, indicating their alike electrochemical behavior (two electrons reaction process). However, there are some slight difference in the peak intensity and enclosed area of CV curves. As comparison

with PDMA-n, the redox peak intensities at different scan rate of PDMA-x and PDMA-t are slight higher than these of PDMA-n at corresponding scan rate, indicating the high electrochemical activity of PDMA-x and PDMA-t resulted from their uniform morphologies. At the meanwhile, the peak area enclosed by the CV curves of PDMA-x and PDMA-t are larger than these of PDMA-n, implying more accessible redox sites of PDMA-x and PDMA-t contributing from their nanostructure. The area of CV curve is proportional to the exchanged charge volume of active materials, so a better capacitive performance of PDMA-t based electrode is expectable since that it has largest area among three samples.

The charge–discharge test at a constant current is the major method for studying the capacitive properties of supercapacitors. According the equation,[18] the specific capacitance is proportional to the discharge time. Figure 6 shows the charge–discharge curves of PDMA-n, PDMA-x, and PDMA-t at different current densities from 5 mA cm^{-2} to 50 mA cm^{-2}. Unlike to the triangular charge–discharge curves of carbon based double layer capacitors, there are two charge plats and two discharge plats in the conducting polymer based pseudo-capacitors, indicating the two redox reactions of PDMA during the charge–discharge process. The specific capacitance of PDMA-n, PDMA-x, and PDMA-t at different current densities are calculated and listed in Table I. At all current densities, the PDMA-x and PDMA-t exhibits superior specific capacitance over those of PDMA-n. Especially at current density of 50 mA cm^{-2}, PDMA-t has 59% and 28% enhancement in specific capacitance in comparison with those of PDMA-n and PDMA-x, respectively, indicating the better rate performance of interfacial polymerized PDMA. At other current densities, PDMA-t and PDMA-x also has better specific capacitance over that of PDMA-n to some extent. Though the performance of PDMA-x is better that PDMA-n, it is worse than PDMA-t owing to its larger aggregation size and lower mesoporoes volume.

The value of another two key parameters for practical application of supercapacitors, the energy density and power density at different current densities are listed in Table I. It can be found that the energy densities of PDMA-t and PDMA-x are higher than that of PDMA-n, which means that the energy storage capacity of PDMA-t and PDMA-x are better than that of PDMA-n. The enhanced capacitive performances can be benefited from the uniform morphology of interfacial polymerized PDMA. In an interfacial polymerization system with organic phase at the bottom, the produced PDMA has a light density (lighter than water) and uniform morphology owing to the flotation function of above water phase. The relative loose packing structure (light density and high pore volume) and uniform morphology are helpful for increasing the ions diffusion depth into the electrode materials during the charge–discharge process, improving the electrochemical activity of PDMA, as well as reinforcing the capacitive properties.

CONCLUSIONS

The PDMA with uniform nanoparticles structure were synthesized successfully through interfacial polymerization approach. The morphologies and uniformity of PDMA particles are dependant on the organic solvent/water system employed. The carbon tetrachloride/water system produces uniform PDMA nanoparticle. The difference in the morphology can affect the electrochemical behavior of PDMA. The PDMA synthesized by interfacial polymerization exhibits facile redox process and larger charge–discharge volume as comparison with conventional PDMA. Also, the better capacitive performances of PDMA-t are obtained. The interfacial polymerization method is easy for large scale production of conducting polymer nanomaterials with good electrochemical activity, which may have potential application in enhancement of the performance of various types of electrochemical devices that require materials morphologies.

ACKNOWLEDGMENTS

The authors thank the National Natural Science Foundation of China (Grant No. 51373134), Opening Project of State Key Laboratory of Polymer Materials Engineering (Sichuan University) (KF201209) and Scientific Research Program funded by Shaanxi Provincial Education Department (Program No. 11JK0833) for the financial support of this work.

REFERENCES

1. Snook, G. A.; Kao, P.; Best, A. S. *J. Power Sources*. **2011**, *196*, 1.
2. Bélanger, D.; Ren, X.; Davey, J.; Uribe, F.; Gottesfeld, S. *J. Electrochem. Soc.* **2000**, *147*, 2923.
3. Xiong, S.; Yang, F.; Jiang, H.; Ma, J.; Lu, X. *Electrochimica Acta* **2012**, *85*, 235.
4. Reddy, K. R.; Jeong, H. M.; Lee, Y.; Raghu, A. V. *J. Polym. Sci. Part A: Polym. Chem.* **2010**, *48*, 1477.
5. Zhang, H.; Li, H.; Zhang, F.; Wang, J.; Wang, Z.; Wang, S. *J. Mater. Res.* **2008**, *23*, 2326.
6. Ganesan, R.; Shanmugam, S.; Gedanken, A. *Synth. Met.* **2008**, *158*, 848.
7. Zhao, G.; Li, H. *Micro. Meso. Mater.* **2008**, *110*, 590.
8. Chaudhari, S.; Sharma, Y.; Archana, P. S.; Jose, R.; Ramakrishna, S.; Mhaisalkar, S.; Srinivasan, M. *J. Appl. Polym. Sci.* **2013**, *129*, 1660.
9. Huang, J.; Virji, S.; Weiller, B. H.; Kaner, R. B. *Chem. Eur. J.* **2004**, *10*, 1314.
10. Huang, J.; Kaner, R. B. *Angew. Chem. Int. Ed.* **2004**, *43*, 5817.
11. Huang, J.; Kaner, R. B. *Chem. Commun.* **2006**, *4*, 367.
12. Gupta, B.; Prakash, R. *Macromol. Chem. Phys.* **2012**, *213*, 1457.
13. Joshi, L.; Singh, A. K.; Prakash, R. *Macromol. Chem. Phys.* **2012**, *80*, 135.
14. Gupta, B.; Prakash, R. *Synth. Met.* **2010**, *160*, 523.
15. Lai, Y.; Lu, H.; Zhang, Z.; Li, J.; Li, J.; Liu, Y. *Zhongnan Daxue Xuebao (Ziran Kexue Ban)/J. Central South University (Science and Technology)* **2007**, *38*, 1110.
16. Palaniappan, S. P.; Gnanakan, S. R. P.; Lee, Y. S.; Manisankar, P. *Ionics* **2011**, *17*, 603.
17. Patil, D.; Seo, Y.-K.; Hwang, Y. K.; Chang, J.-S.; Patil, P. *Sens Actuators B* **2008**, *132*, 116.
18. Meyyappan, M. Carbon Nanotubes Science and Applications; CRC Press: Boca Raton, FL, **2004**.